Research Square

Preprints are preliminary reports that have not undergone peer review.
They should not be considered conclusive, used to inform clinical practice,
or referenced by the media as validated information.

Myeloid Immune Remodeling Associated With Citrullination-Related Candidate Markers in Sepsis From a Single-Cell Perspective

Jingjie Wang
Xinjiang Medical University
Xiang Li
Xinjiang Medical University
Jingyan Wang
Xinjiang Medical University
Xiangyou Yu
First Affiliated Hospital of Xinjiang Medical University
Hanyu Zhao
Xinjiang Medical University
Di Nie
Xinjiang Medical University
Chunbo Yang
First Affiliated Hospital of Xinjiang Medical University
Zhihua Li
First Affiliated Hospital of Xinjiang Medical University
Yi Wang
icuwangyi@163.com

First Affiliated Hospital of Xinjiang Medical University

Research Article

Keywords: sepsis, citrullination, single-cell analysis, cell-cell communication, immune infiltration

Posted Date: July 24th, 2026

DOI: https://doi.org/10.21203/rs.3.rs-9811289/v1

License: This work is licensed under a Creative Commons Attribution 4.0 International License.
Read Full License

Additional Declarations: No competing interests reported.

Abstract

Background

Sepsis is characterized by profound immune dysregulation, but the cellular distribution and immunological relevance of citrullination-related candidate biomarkers remain incompletely understood. This study aimed to define the single-cell localization of six candidate biomarkers and explore their relationship with myeloid immune remodeling in sepsis.

Methods

The single-cell RNA-seq dataset GSE167363 and the bulk transcriptomic dataset GSE185263 were integrated for analysis. Immune cell annotation, myeloid subcluster analysis, pseudotime trajectory inference, CellChat-based cell-cell communication analysis, and immune infiltration correlation analysis were performed to evaluate the expression distribution and potential immune relevance of LTF, MMP9, MMP8, IL10, LCN2, and S100A12.

Results

The six candidate biomarkers were mainly localized to myeloid cells. LTF, MMP9, MMP8, LCN2, and S100A12 were closely associated with neutrophils, whereas IL10 was enriched in CD14 + + monocytes/macrophages. Myeloid cells showed prominent differences in cellular composition and communication patterns between sepsis and control samples. Pseudotime analysis further suggested dynamic transcriptional states across myeloid subpopulations, and immune infiltration analysis supported broad associations between candidate biomarkers and myeloid-dominated immune remodeling.

Conclusions

These findings provide cellular-level evidence that citrullination-related candidate biomarkers are linked to neutrophil effector activation and monocyte/macrophage immune regulatory programs in sepsis. The results support further validation of these markers as potential indicators of myeloid immune remodeling.

Background

Sepsis is defined as life-threatening organ dysfunction caused by a dysregulated host response to infection[1]. Severe sepsis is associated with a mortality rate of approximately 26% [2] and remains one of the leading causes of in-hospital death. Globally, an estimated 31.5 million new cases of sepsis occur each year, resulting in up to 5.3 million deaths[3]. The pathogenesis of sepsis remains incompletely

understood and involves multiple processes, including immune cell imbalance and cytokine storm. Current therapeutic strategies have not fully addressed immune dysregulation, and targeted approaches directed at disease-relevant immune cell populations remain limited. Single-cell RNA sequencing (scRNA-seq) enables high-resolution analysis of gene expression at the individual-cell level, accurate identification and classification of cell subpopulations, and characterization of cellular heterogeneity. By analyzing cellular differentiation, evolution, and response mechanisms across disease states, scRNA-seq provides an important tool for understanding immune responses, identifying disease-associated molecular features, and exploring cell-type-specific therapeutic implications[4].

Based on this rationale, the present study integrated the sepsis single-cell dataset GSE167363 and the bulk transcriptomic dataset GSE185263 to characterize immune cell composition during sepsis progression. We further performed dimensionality reduction and clustering analyses of key immune cells, explored candidate gene expression, constructed single-cell trajectories, and analyzed dynamic gene expression trends, thereby providing a theoretical basis for immune stratification, mechanistic investigation, and potential intervention strategies in sepsis.

Methods

Data Collection

The sepsis bulk transcriptomic dataset GSE185263 and the single-cell dataset GSE167363 were downloaded from the NCBI Gene Expression Omnibus (GEO; https://www.ncbi.nlm.nih.gov/). The corresponding platform annotation files were also obtained for downstream analysis. The datasets used in this study are summarized in Table 1. This study was based on publicly available datasets from the GEO database. No new human samples were collected, and no individual-level identifiable information was used. Therefore, additional ethical approval and informed consent were not required.

Table 1
Summary of Transcriptomic and Single-Cell RNA-Seq Datasets Used

ID	Type	Disease	Control	Platform
GSE185263	transcriptome	348	44	GPL16791Illumina HiSeq 2500 (Homo sapiens)
GSE167363	single-cell	10	2	GPL24676Illumina NovaSeq 6000 (Homo sapiens)

Source of Biomarkers

The citrullination-related biomarkers included in this study were derived from our previous multi-omics integrative analysis. Briefly, citrullination-related genes were collected from the GeneCards database using the keywords "Citrullination", "PADI2", and "PADI4". Differentially expressed genes between sepsis and normal control samples were identified in the GSE185263 training dataset using DESeq2, and sepsis

phenotype-associated module genes were obtained by weighted gene co-expression network analysis (WGCNA). Candidate genes were obtained by intersecting differentially expressed genes, sepsis-related module genes, and citrullination-related genes. A protein-protein interaction network was then constructed using the STRING database and Cytoscape cytoHubba plugin to identify key genes. Subsequently, 113 model combinations derived from 12 machine learning algorithms were used for feature selection and diagnostic model construction, and the expression trends and diagnostic performance of selected genes were validated in independent datasets. Finally, LTF, MMP9, MMP8, IL10, LCN2, and S100A12 were identified as citrullination-related candidate biomarkers in sepsis. On this basis, the present study further investigated their cellular sources, distribution across myeloid cell subpopulations, pseudotime dynamics, and cell-cell communication features using single-cell transcriptomic data.

Single-Cell RNA-Seq Processing and Cell Annotation

To obtain high-quality cells and genes, the single-cell dataset was filtered using the Seurat package (v5.0.1). The data were first normalized using the NormalizeData function in Seurat. Highly variable genes were then identified using FindVariableFeatures, and the top 2,000 genes with the greatest intercellular variation were selected for downstream analyses. The data were scaled using ScaleData. Statistically significant principal components were evaluated using JackStrawPlot, and the top highly variable genes were used for principal component analysis with RunPCA. ElbowPlot was used to determine the appropriate dimensionality, and JackStraw was used for permutation-based assessment of significant principal components. Principal components with statistical significance ($P < 0.05$) were selected for subsequent clustering. Batch effects were corrected using Harmony. A shared nearest neighbor graph was constructed based on the selected PCs, followed by Louvain clustering at a resolution of 0.2. Uniform manifold approximation and projection (UMAP) was used for further dimensionality reduction. Marker genes for specific clusters were identified using FindAllMarkers in Seurat with a log2 fold-change threshold greater than 0.25 and $P < 0.05$. Cell types were manually annotated with reference to established resources, including PanglaoDB and CellMarker 2.0, and the proportions of different cell types across samples were visualized. GO and KEGG enrichment analyses were then performed for annotated cell populations to explore their biological functions. UMAP plots were used to display the distribution of candidate biomarkers across cell types. Based on biomarker expression distribution, changes in cell composition, and cell-cell communication network characteristics, myeloid cells were selected as the key cell population for further analysis.

Cell-Cell Communication Analysis

To investigate interactions among all cell populations, cell-cell communication analysis was performed separately in the disease and control groups using the CellChat R package (version 1.6.1; https://github.com/jinworks/CellChat). Normalized single-cell gene expression data were used as input, and communication probabilities were inferred by integrating gene expression with prior knowledge of

ligand-receptor interactions. CellChat was used to infer communication probabilities between cell groups based on its built-in ligand-receptor database, and differences between the disease and control groups were compared in terms of communication number, communication strength, and major signaling pathways. Cell interaction network plots were constructed to illustrate regulatory relationships among cell populations.

Heterogeneity Analysis of Key Cells

To clarify the heterogeneity of key cells, myeloid cells were extracted from the single-cell dataset and subjected to dimensionality reduction and reclustering to identify distinct subpopulations. Marker genes of different myeloid subclusters were identified using FindAllMarkers with the parameters min.pct = 0.5, logfc.threshold = 0.25, and test.use = "auc". These marker genes were compared with known markers in the CellMarker database to determine the identity of each subpopulation, and the expression patterns of subcluster marker genes were visualized. After identifying myeloid subpopulations, Monocle was used to infer differentiation relationships, cellular trajectories, and pseudotime. Monocle2 (v2.36.0) was applied to project all myeloid subclusters onto a trajectory with a root and multiple branches. The presence of distinct trajectories was interpreted as evidence of transcriptional heterogeneity within myeloid cells. To explore the expression patterns of biomarkers across different transcriptional states, the BEAM method in Monocle was used to assess stage-associated gene expression and reveal dynamic trends during pseudotime progression.

Immune Infiltration Analysis

To explore immune cell infiltration in the sepsis and control groups, the CIBERSORT algorithm, implemented with the e1071 (v1.7-13) and preprocessCore (v1.56.0) R packages, was used to estimate immune cell proportions in the sepsis training set. The Wilcoxon test was used to identify immune cell types that differed significantly between groups ($P < 0.05$), which were defined as differentially infiltrating immune cells. Spearman correlation analysis was then performed to evaluate associations between biomarkers and differentially infiltrating immune cells. Correlation results were visualized as heatmaps using the pheatmap package (v1.0.12; https://cran.r-project.org/web/packages/pheatmap/index.html).

Results

Single-Cell Landscape of Sepsis: Quality Control and Cell Annotation

Quality control was performed on the sepsis single-cell dataset. Cells with fewer than 200 detected genes, genes expressed in fewer than three cells, cells with fewer than 200 or more than 6,000 detected genes, cells with a mitochondrial gene percentage greater than 10%, and cells with an erythrocyte gene percentage greater than 5% were filtered out (Fig. 1A,B). After quality control, the single-cell dataset was

annotated. Before annotation, 15 clusters were identified (Fig. 1C). After annotation using marker genes, the cells were classified into six major cell types: T cells, myeloid cells, B cells, NK cells, platelets, and erythroid cells (Fig. 1D). The top 2,000 highly variable genes (Fig. 1E) were selected for principal component analysis, and the top 30 principal components were used for downstream analysis (Fig. 1F). A dot plot was used to display the expression of cell-subtype marker genes across different cell clusters (Fig. 1G). We further analyzed the expression of marker genes across cell clusters and the proportions of different cell types in sepsis and control samples. Myeloid cells accounted for the highest proportion in the sepsis group, whereas T cells accounted for the highest proportion in the control group (Fig. 1H).

GO and KEGG Enrichment Analyses

GO and KEGG enrichment analyses were performed for all annotated cell populations to explore their biological pathways(Fig. 2). In T cells, enriched GO terms(Fig. 2A) included cytoplasmic translation (BP), ribosome (CC), structural constituent of ribosome (MF), ribosomal subunit (CC), cytosolic ribosome (CC), ribonucleoprotein complex biogenesis (BP), large ribosomal subunit (CC), cytosolic large ribosomal subunit (CC), small ribosomal subunit (CC), and cytosolic small ribosomal subunit (CC). Enriched KEGG(Fig. 2B) pathways included Coronavirus disease-COVID-19, human T-cell leukemia virus 1 infection, Th17 cell differentiation, measles, and the T-cell receptor signaling pathway. In myeloid cells, enriched GO terms included focal adhesion (CC), cell-substrate junction (CC), vesicle lumen (CC), cytoplasmic vesicle lumen (CC), and secretory granule lumen (CC). Enriched KEGG pathways included pathways of neurodegeneration-multiple diseases, Alzheimer disease, amyotrophic lateral sclerosis, Parkinson disease, and Huntington disease.

Cell-Cell Communication Analysis

Further analysis of cell-cell communication showed that, after quantifying the number and strength of interactions, both the interaction number and interaction strength were higher in the normal group than in the sepsis group (Fig. 3A). Comparison of communication number and strength among different cell types showed that interactions between myeloid cells and B cells were the most frequent and strongest in both the normal and sepsis groups (Fig. 3B). Analysis of key receptor-ligand interactions and potential intercellular communication relationships within the immune system revealed that active receptor-ligand pairs such as CD99-CD99 and HLA-DRA-CD4 were widely present in myeloid cell to myeloid cell communication in the normal group, whereas RETN-CAP1 was widely present in myeloid cell to myeloid cell communication in the sepsis group (Fig. 3C,D). Further visualization of communication signaling networks in the normal and sepsis groups showed multiple pathways, including MIF, MHC-I, MHC-II, CD99, CLEC, and GALECTIN. Overall, myeloid cells exhibited a denser and more broadly connected signaling network and were therefore identified as the key cell population. Based on previous screening results, LTF, MMP9, MMP8, IL10, LCN2, and S100A12 were selected as citrullination-related candidate biomarkers, and their expression distribution in the GSE167363 single-cell dataset was further analyzed.

Single-Cell Myeloid Cell Trajectory Analysis in Sepsis: Cell-Type Annotation, Hub Gene Localization, and Pseudotime Dynamics

For the key cell population, myeloid cells were extracted and analyzed based on their gene expression profiles using dimensionality reduction and clustering. As shown in Fig. 4A, 10 clusters were identified before annotation. After annotation using marker genes, four distinct subtypes were identified: CD14 + + monocytes/macrophages, neutrophils, CD14 + monocytes/macrophages, and dendritic cells (DCs). Six key genes, LTF, MMP9, MMP8, LCN2, S100A12, and IL10, were visualized (Fig. 4C). LTF, MMP9, MMP8, LCN2, and S100A12 were highly expressed in neutrophils, whereas IL10 was highly expressed in CD14 + + monocytes/macrophages. A dot plot was used to display the expression of these key genes across the four myeloid subtypes (Fig. 4D).

Pseudotime Analysis of Myeloid Cell Subtypes and Dynamic Gene Expression

To investigate gene expression dynamics during changes in myeloid cell states, pseudotime analysis was performed using the “Monocle2” R package. As shown in Fig. 5A, in myeloid cells, cells started from State 1, which was mainly composed of neutrophils and located on the right side of the trajectory. Cells then progressed toward States 2 and 5, which were mainly composed of CD14 + + monocytes/macrophages, CD14 + monocytes/macrophages, and DCs, and finally toward States 3 and 4. As shown in Fig. 5B, LCN2, MMP8, and MMP9 showed a trend of initial decrease, relative stabilization, and subsequent increase along pseudotime. IL10 remained relatively stable at the beginning, then fluctuated, and finally showed an increasing trend. LTF initially decreased and then remained relatively stable, whereas S100A12 showed an initial decrease followed by a later increase.

Immune Infiltration Analysis

To characterize immune cell infiltration patterns in patients with sepsis and normal controls, immune infiltration analysis was performed to estimate the proportion of each immune cell type in every sepsis sample (Fig. 6A,B). The psych R package was further used to analyze correlations between immune cells and key genes in the sepsis training set (Fig. 6C,D). For example, S100A12 showed significant positive correlations with naive B cells, naive CD4 T cells, gamma delta T cells, M0 macrophages, M2 macrophages, activated dendritic cells, activated mast cells, and neutrophils, suggesting potential associations with enhanced immune cell activity. In contrast, S100A12 showed significant negative correlations with memory B cells, plasma cells, CD8 T cells, resting memory CD4 T cells, regulatory T cells, resting NK cells, activated NK cells, monocytes, M1 macrophages, and resting dendritic cells, suggesting potential associations with altered or suppressed immune cell functions.

Discussion

Sepsis is a life-threatening organ dysfunction caused by a dysregulated host response to infection[2]. It causes substantial morbidity and mortality worldwide, and sepsis accounted for 31.5% of global deaths in 2021. Although clinical guidelines for sepsis have been continuously updated and strategies such as fluid resuscitation, antimicrobial therapy, organ support, and source control have become increasingly standardized, early identification, immune status assessment, and precise stratification remain challenging because of the acute onset, rapid progression, and marked clinical heterogeneity of sepsis[5]. Recent global burden studies indicate that sepsis remains associated with high incidence and mortality worldwide, and its disease burden extends beyond acute-phase mortality to include long-term organ dysfunction, immune abnormalities, and increased risk of readmission[5]. Pathophysiologically, sepsis is not driven by a single inflammatory mediator but rather by a dynamic imbalance involving both innate and adaptive immunity, with concomitant hyperinflammation and immunosuppression[6, 7]. Myeloid cells, including neutrophils, monocytes, macrophages, and dendritic cells, play central roles in this process by recognizing pathogens, clearing infections, releasing inflammatory mediators, regulating coagulation, and initiating antigen presentation[8, 9]. In early sepsis, neutrophils are rapidly recruited and undergo chemotaxis, degranulation, phagocytosis, and neutrophil extracellular trap formation, thereby enhancing antimicrobial defense[10]. However, excessive activation or insufficient clearance of neutrophils can amplify inflammation and induce endothelial injury, microcirculatory dysfunction, coagulation abnormalities, and multiple organ dysfunction[11]. Meanwhile, monocytes/macrophages can release pro-inflammatory mediators but may also contribute to immunosuppression and immunoparalysis through anti-inflammatory cytokine release, reduced antigen presentation, and decreased HLA-DR expression[12]. Therefore, single-cell-level characterization of myeloid cell composition, state transitions, and key molecular expression may help elucidate the cellular basis of immune remodeling in sepsis.

Citrullination is a post-translational modification mediated by peptidylarginine deiminases, in which arginine residues are converted into citrulline residues. This modification alters protein charge, structure, and immunogenicity and plays important roles in inflammatory regulation, autoimmunity, and neutrophil function[13]. During sepsis, PAD4-mediated histone citrullination promotes chromatin decondensation and neutrophil extracellular trap formation, and citrullinated histone H3 (CitH3) has been regarded as an important marker of NETosis activation[14]. Based on six citrullination-related candidate markers identified in our previous analysis, the present study further investigated their cellular localization and immunological relevance from a single-cell perspective. LTF, MMP8, MMP9, LCN2, and S100A12 were mainly enriched in neutrophil subpopulations. These molecules are closely related to neutrophil degranulation, antimicrobial responses, extracellular matrix remodeling, inflammatory amplification, and tissue injury, suggesting that their high expression may reflect enhanced neutrophil effector programs in sepsis. S100A12, a member of the S100 calcium-binding protein family, can amplify inflammatory signaling through receptors such as RAGE and has been associated with sepsis-related organ injury[15]. MMP8 and MMP9 are involved in matrix degradation, tissue infiltration, and inflammation-mediated extracellular matrix remodeling[16, 17]. LCN2, also known as NGAL, is commonly regarded as an important molecule associated with infection, inflammation, and sepsis-associated acute kidney

injury[18]. In contrast to these neutrophil-associated molecules, IL10 was mainly enriched in CD14 + + monocyte/macrophage subpopulations, suggesting the concurrent activation of anti-inflammatory feedback and immune braking programs during myeloid immune remodeling in sepsis[7]. These results indicate that citrullination-related candidate markers are not uniformly distributed across all immune cells but are primarily mapped to distinct functional states within the myeloid compartment.

Further cell-cell communication analysis demonstrated marked alterations in interaction patterns among immune cells under septic conditions. Myeloid cells displayed dense signaling connections within the communication network, suggesting that they serve not only as major sources of inflammatory effector molecules but also as important mediators of immune regulatory signaling. The development of single-cell transcriptomics has provided new approaches for deciphering intercellular communication. Tools such as CellChat infer potential signaling inputs and outputs among cell populations based on ligand-receptor expression[19, 20].In this study, differences in communication number, communication strength, and ligand-receptor interaction patterns were observed between the normal and sepsis groups, with myeloid cell-related communication occupying a central position in both groups. In the normal group, interactions such as CD99-CD99 and HLA-DRA-CD4 were prominent, suggesting that antigen presentation, cell adhesion, and maintenance of immune homeostasis may represent key features of myeloid communication under healthy conditions. In the sepsis group, enhanced RETN-CAP1 interactions suggested that inflammatory mediator release, myeloid cell activation, and metabolic stress-related signaling may participate in disease-associated immune remodeling. Previous single-cell studies have also shown that antigen-presenting cells, monocytes, and dendritic cells exhibit functional imbalance in sepsis, characterized by coexistence of immune activation and immune anergy[21, 22]. In addition, changes in MIF, MHC-I, MHC-II, CD99, CLEC, and GALECTIN pathways further indicate that myeloid cell communication in sepsis is not a single pro-inflammatory process but involves antigen presentation, chemotaxis, cell adhesion, inflammatory regulation, and immunosuppression. Together with the expression distribution of the candidate markers in neutrophils and monocytes/macrophages, these findings suggest that citrullination-related candidate markers may be embedded in myeloid cell-dominated communication networks and may participate in remodeling of the septic immune microenvironment by influencing intercellular inflammatory signaling.

Myeloid cells are not functionally homogeneous but exhibit substantial state heterogeneity across different stages of sepsis. Previous single-cell studies have demonstrated the presence of disease-associated CD14 + monocyte states in peripheral immune cells from patients with sepsis, and these states can help distinguish infectious inflammation from healthy conditions, indicating that single-cell approaches can reveal cell states that are difficult to resolve using bulk transcriptomic data[23]. In the present study, reclustering of myeloid cells identified four subpopulations: CD14 + + monocytes/macrophages, neutrophils, CD14 + monocytes/macrophages, and DCs. These findings suggest that sepsis-associated myeloid immune abnormalities involve enhanced neutrophil effector programs, inflammatory regulation by monocytes/macrophages, and altered antigen presentation by DCs. Pseudotime analysis further showed that these myeloid subpopulations were continuously distributed and branched across transcriptional states, suggesting that myeloid cells in sepsis may

transition from acute inflammatory effector states toward immune regulatory or antigen presentation-related states. Importantly, pseudotime analysis reflects the relative ordering of cellular transcriptional states and should not be interpreted as evidence of strict lineage differentiation. Therefore, we interpreted these results as dynamic changes in myeloid functional states. Under the root setting used in this study (pseudotime = 0),different myeloid subpopulations showed branched distributions along pseudotime, suggesting that neutrophil effector states, monocyte/macrophage regulatory states, and DC-associated antigen presentation states may represent distinct transcriptional-functional states of myeloid cells in sepsis. However, because pseudotime analysis cannot be directly equated with real temporal progression or lineage differentiation, these state transitions require further validation by functional experiments. Combined with the pseudotime expression trends of key genes, neutrophil-associated molecules such as LCN2, MMP8, MMP9, and S100A12 showed dynamic fluctuations across different states, suggesting that degranulation, matrix remodeling, and inflammatory amplification programs may be dynamically regulated according to disease course or immune status. In contrast, stage-dependent increases in IL10 may indicate gradual enhancement of anti-inflammatory feedback and immunosuppressive signaling during myeloid state transitions. These findings are consistent with the coexistence of hyperinflammation and immunosuppression in sepsis and support the need to understand sepsis immune heterogeneity through myeloid cell states rather than relying on a single inflammatory marker[24].

To further validate the single-cell findings, immune infiltration analysis was performed using the bulk sepsis transcriptomic dataset GSE185263. The results showed significant differences in the proportions of multiple immune cell types between the sepsis and normal control groups, suggesting extensive remodeling of the immune microenvironment in sepsis. Changes in myeloid-related cells, including neutrophils, monocytes, macrophages, and dendritic cells, were consistent with the increased proportion of myeloid cells, enhanced communication network features, and increased subpopulation heterogeneity observed in the single-cell analysis. Further correlation analysis showed that candidate markers such as S100A12 were significantly associated with infiltration levels of neutrophils, macrophages, dendritic cells, and other immune cell types, suggesting that these markers may not only serve as disease-associated expression features but may also reflect changes in immune cell composition and functional status in sepsis. Notably, immune infiltration analysis based on bulk transcriptomic data reflects the overall signal of mixed cell populations, whereas single-cell analysis provides a more refined explanation of cellular sources. Integrating these two approaches helps clarify the biological significance of citrullination-related markers at both the global immune microenvironment and single-cell levels. Recent studies increasingly support sepsis risk stratification based on immune cell proportions, inflammatory mediators, injury markers, and transcriptomic features, suggesting that future sepsis research should move from single diagnostic biomarkers toward immune phenotype stratification and identification of actionable targets[25]. Overall, our findings suggest that LTF, MMP8, MMP9, LCN2, S100A12, and IL10 may not merely represent diagnostic molecules but may also be closely associated with myeloid cell-driven inflammatory amplification, immune regulation, cell-cell communication remodeling, and NETosis-related processes.

This study has several limitations. First, both the single-cell and bulk transcriptomic datasets were obtained from public databases, which may affect the generalizability of the findings. Second, although LTF, MMP8, MMP9, LCN2, S100A12, and IL10 were analyzed as citrullination-related candidate markers, their relationships with citrullination modification, CitH3 levels, and NETosis activation were inferred mainly from database screening and transcriptomic associations; direct validation at the protein level and functional experiments are still lacking. Third, pseudotime analysis reflects relative continuity in transcriptional states and cannot prove true lineage transitions among myeloid subpopulations. Fourth, cell-cell communication analysis infers potential interactions based on ligand and receptor transcript levels, and experimental validation remains necessary. Future studies should combine in vivo and in vitro functional experiments to validate the dynamic changes and functional roles of candidate markers across different immune stages.

Conclusions

This study found that LTF, MMP8, MMP9, LCN2, and S100A12 were mainly enriched in neutrophils, reflecting enhanced effector programs such as degranulation, protease release, tissue infiltration, and inflammatory amplification. IL10 was mainly enriched in CD14 + + monocytes/macrophages, suggesting activation of anti-inflammatory feedback and immune braking programs and revealing a structured imbalance characterized by the coexistence of pro-inflammatory effector responses and immunosuppression in sepsis. Different immune states may correspond to distinct disease stages and clinical phenotypes, providing a theoretical basis and candidate targets for subsequent protein-level validation, mechanistic studies, and exploration of therapeutic strategies targeting myeloid effector programs and NET-related pathways.

Declarations

Ethics approval and consent to participate

This study was based exclusively on publicly available datasets from the Gene Expression Omnibus database. No new human samples were collected, and no individual-level identifiable information was used. Therefore, additional ethics approval and informed consent were not required.

Consent for publication

Not applicable.

Competing interests

The authors declare that the research was conducted in the absence of any commercial or financial relationships that could be construed as a potential conflict of interest.

Author Contribution

Jingjie Wang, Xiang Li, Jingyan Wang, Zhihua Li designed the study; Jingjie Wang, Jingyan Wang, Xiang Li retrieved the data; Jingjie Wang, Jingyan Wang, Xiang Li wrote the manuscript. All authors affirm their contributions to the manuscript reviews, involving critical revisions for significant intellectual content, and their approval of the final text for submission. Every author bears the responsibility for the content of the manuscript.

Acknowledgements

Not applicable.

Availability of data and materials

The datasets analyzed in this study are publicly available in the GEO database under accession numbers GSE185263 and GSE167363.

References

1. Singer M, Deutschman CS, Seymour CW, Shankar-Hari M, Annane D, Bauer M, et al. The third international consensus definitions for sepsis and septic shock (sepsis-3). JAMA. 2016;315:801–10. https://doi.org/10.1001/jama.2016.0287.
2. Prescott HC, Antonelli M, Alhazzani W, Møller MH, Alshamsi F, Azevedo LCP, et al. Surviving sepsis campaign: international guidelines for management of sepsis and septic shock 2026. Intensive Care Med. 2026. https://doi.org/10.1007/s00134-026-08361-1.
3. Fleischmann C, Scherag A, Adhikari NKJ, Hartog CS, Tsaganos T, Schlattmann P, et al. Assessment of global incidence and mortality of hospital-treated sepsis. Current estimates and limitations. Am J Respir Crit Care Med. 2016;193:259–72. https://doi.org/10.1164/rccm.201504-0781OC.
4. Darden DB, Dong X, Brusko MA, Kelly L, Fenner B, Rincon JC, et al. A novel single cell RNA-seq analysis of non-myeloid circulating cells in late sepsis. Front Immunol. 2021;12:696536. https://doi.org/10.3389/fimmu.2021.696536.
5. Gray AP, Chung E, Hsu RL, Araki DT, Hayoon AG, Weaver ND, et al. Global, regional, and national sepsis incidence and mortality, 1990–2021: a systematic analysis. Lancet Glob HEALTH Elsevier. 2025;13:e2013–26. https://doi.org/10.1016/S2214-109X(25)00356-0.
6. Venet F, Monneret G. Advances in the understanding and treatment of sepsis-induced immunosuppression. Nat Rev Nephrol. 2018;14:121–37. https://doi.org/10.1038/nrneph.2017.165.
7. Liu D, Huang S-Y, Sun J-H, Zhang H-C, Cai Q-L, Gao C, et al. Sepsis-induced immunosuppression: Mechanisms, diagnosis and current treatment options. Mil Med Res. 2022;9:56. https://doi.org/10.1186/s40779-022-00422-y.

8. Zhang J, Shao Y, Wu J, Zhang J, Xiong X, Mao J, et al. Dysregulation of neutrophil in sepsis: recent insights and advances. Cell Commun Signal. 2025;23:87. https://doi.org/10.1186/s12964-025-02098-y.
9. Monneret G, Lafon T, Gossez M, Evrard B, Bodinier M, Rimmelé T, et al. Monocyte HLA-DR expression in septic shock patients: Insights from a 20-year real-world cohort of 1023 cases. Intensive Care Med. 2025;51:1820–32. https://doi.org/10.1007/s00134-025-08110-w.
10. Jia W, Zhang J, Shang Y, Liu S. Multitarget natural compounds taming NETosis: a translational strategy for cancer and inflammatory diseases. Cancer Lett. 2026;636:218103. https://doi.org/10.1016/j.canlet.2025.218103.
11. Retter A, Singer M, Annane D. the NET effect: neutrophil extracellular traps-a potential key component of the dysregulated host immune response in sepsis. Crit Care Lond Engl. 2025;29:59. https://doi.org/10.1186/s13054-025-05283-0.
12. Joshi I, Carney WP, Rock EP. Utility of monocyte HLA-DR and rationale for therapeutic GM-CSF in sepsis immunoparalysis. Front Immunol. 2023;14:1130214. https://doi.org/10.3389/fimmu.2023.1130214.
13. Wang J, Miao J, Zhu P. Insights into the complexities of citrullination: From immune regulation to autoimmune disease. Autoimmun Rev. 2025;24:103734. https://doi.org/10.1016/j.autrev.2024.103734.
14. Chen Y, Tetz ZA, Zeng X, Go SJ, Ouyang W, Lee KE, et al. CitH3, a druggable biomarker for human diseases associated with acute NETosis and chronic immune dysfunction. Pharmaceutics. 2025;17:809. https://doi.org/10.3390/pharmaceutics17070809.
15. Wu F, Hong H, Tian Y, Wang X. Serum S100A12 in the clinical diagnosis of sepsis-induced myocardial dysfunction: an integrated bioinformatics and clinical data analysis. Front Cardiovasc Med. 2025;12:1640788. https://doi.org/10.3389/fcvm.2025.1640788.
16. Liu H, Song Y, Lv Y, Qu F, Shi J. Baseline serum matrix metalloproteinase-8 and 28-day mortality in sepsis at ICU admission. Crit Care Lond Engl. 2026;30:51. https://doi.org/10.1186/s13054-026-05877-2.
17. Fan Y, Moser J, van Meurs M, Kiers D, Sand JMB, Leeming DJ, et al. Neo-epitope detection identifies extracellular matrix turnover in systemic inflammation and sepsis: an exploratory study. Crit Care Lond Engl. 2024;28:120. https://doi.org/10.1186/s13054-024-04904-4.
18. Legrand M, Bagshaw SM, Bhatraju PK, Bihorac A, Caniglia E, Khanna AK, et al. Sepsis-associated acute kidney injury: recent advances in enrichment strategies, sub-phenotyping and clinical trials. Crit Care Lond Engl. 2024;28:92. https://doi.org/10.1186/s13054-024-04877-4.
19. Jin S, Plikus MV, Nie Q. CellChat for systematic analysis of cell-cell communication from single-cell transcriptomics. Nat Protoc. 2025;20:181–219. https://doi.org/10.1038/s41596-024-01045-4.
20. Jin S, Guerrero-Juarez CF, Zhang L, Chang I, Ramos R, Kuan C-H, et al. Inference and analysis of cell-cell communication using CellChat. Nat Commun. 2021;12:1088. https://doi.org/10.1038/s41467-021-21246-9.

21. She H, Tan L, Wang Y, Du Y, Zhou Y, Zhang J, et al. Integrative single-cell RNA sequencing and metabolomics decipher the imbalanced lipid-metabolism in maladaptive immune responses during sepsis. Front Immunol. 2023;14:1181697. https://doi.org/10.3389/fimmu.2023.1181697.
22. Zhang T, Lian G, Fang W, Tian L, Ma W, Zhang J, et al. Comprehensive single-cell analysis reveals novel anergic antigen-presenting cell subtypes in human sepsis. Front Immunol. 2023;14:1257572. https://doi.org/10.3389/fimmu.2023.1257572.
23. Reyes M, Filbin MR, Bhattacharyya RP, Billman K, Eisenhaure T, Hung DT, et al. An immune-cell signature of bacterial sepsis. Nat Med Nat Publishing Group. 2020;26:333–40. https://doi.org/10.1038/s41591-020-0752-4.
24. Coudereau R, Haem Rahimi M, Lukaszewicz A-C, Cour M, Bidar F, Argaud L, et al. Immature neutrophils and myeloid-derived suppressor cells in sepsis: differences in occurrence kinetics. Crit Care Lond Engl. 2024;28:7. https://doi.org/10.1186/s13054-023-04781-3.
25. Van Nynatten LR, Bokhary D, Wong MYS, Wang J, Fero H, McChesney C, et al. Predictive enrichment using biomarkers in studies of critically-ill patients with sepsis: a systematic review. Crit Care Lond Engl. 2025;29:504. https://doi.org/10.1186/s13054-025-05684-1.

Figures

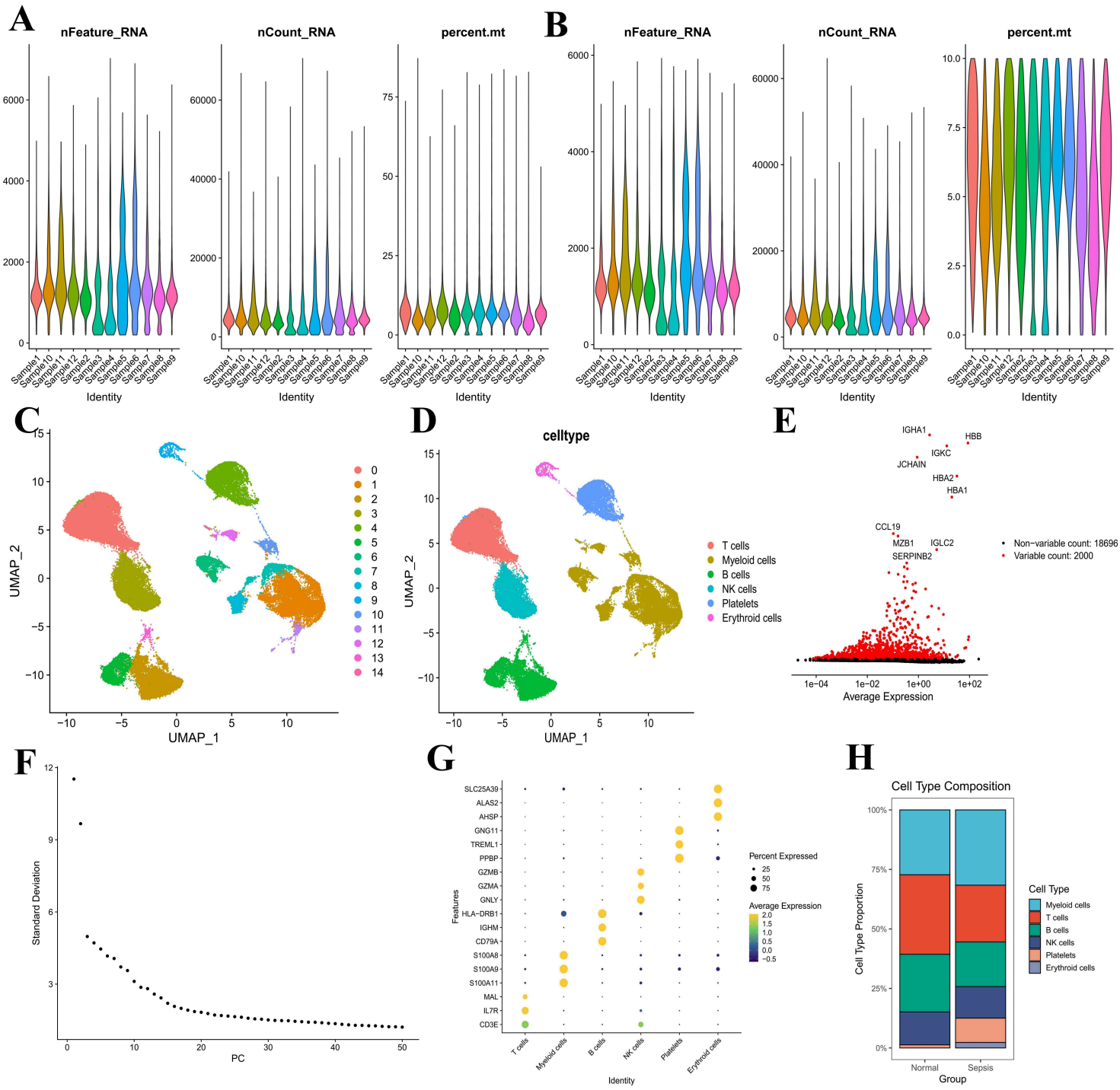


Figure 1

Single-cell RNA sequencing quality control, clustering, and gene expression analysis

A：Violin plots showing the distribution of nFeature_RNA, nCount_RNA, and percent.mt for each cell type before quality control. B：Violin plots showing the same quality control features as in (A), but after applying the quality control filters, excluding low-quality cells. C：UMAP plot of cells colored by cluster identity. D：UMAP plot showing cell type annotations: T cells, Myeloid cells, B cells, NK cells, Platelets, and Erythroid cells. E：Plot showing the relationship between gene expression and variability for highly

variable genes. F Scree plot of standard deviation for each principal component. G Dot plot showing the average expression and percent expression of key marker genes across cell types. H Bar plot depicting the cell type composition in normal and sepsis groups.

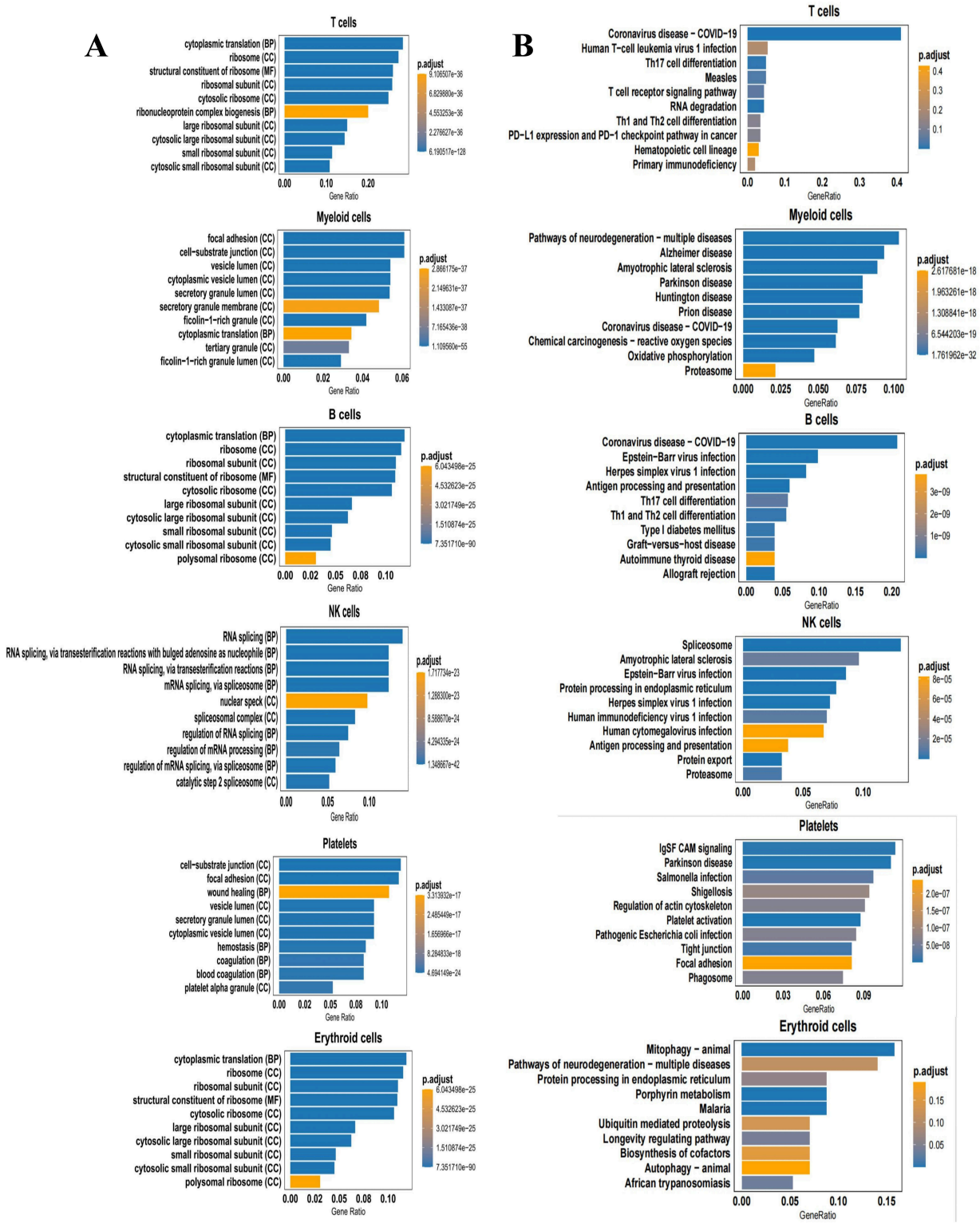


Figure 2

GO and KEGG Enrichment Analysis of Different Immune Cell Types.

A：The top five enriched GO pathways for different immune cell types. B：The top five enriched KEGG pathways for different immune cell types.

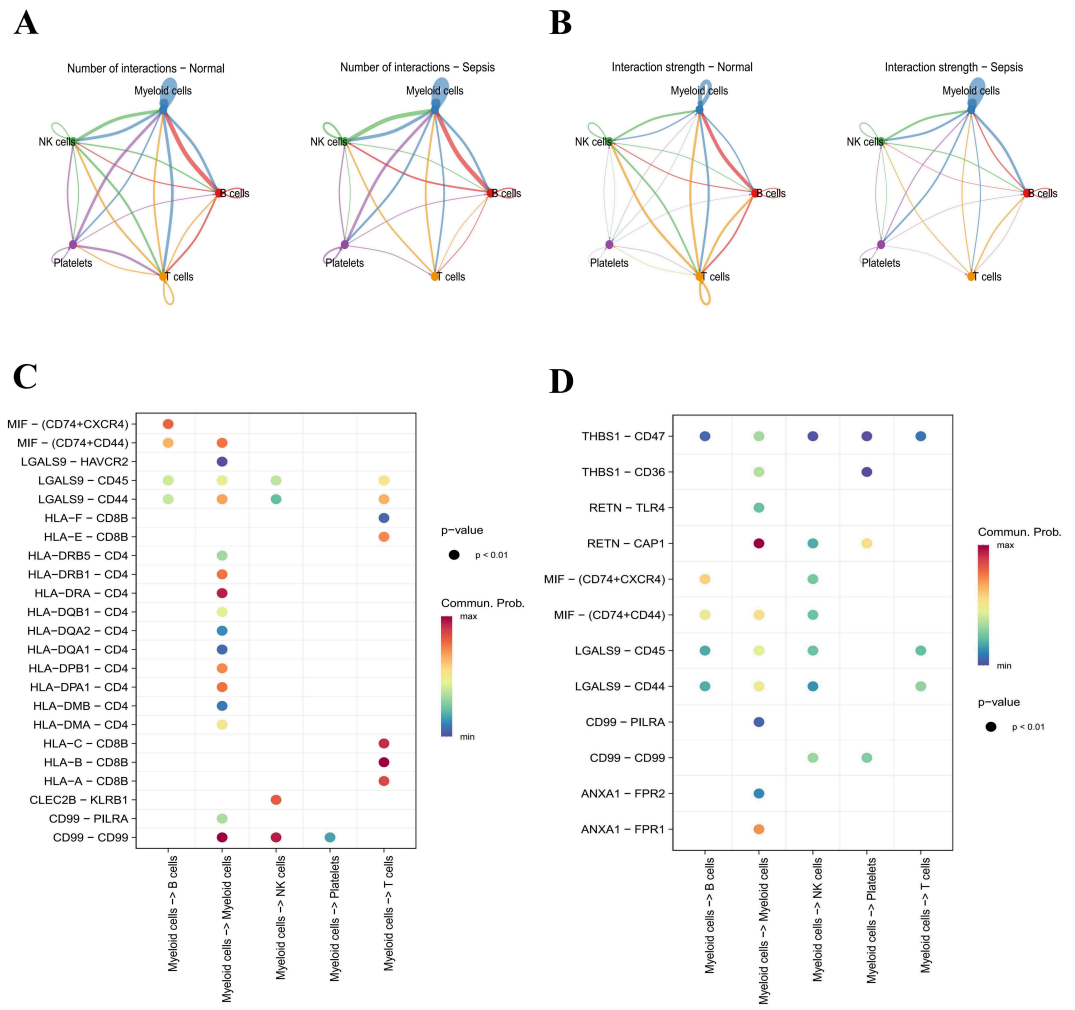


Figure 3

Cell-to-Cell Communication Analysis

A: Cell communication quantity network in the Normal and Sepsis groups. The size of the peripheral colored circles represents the number of cells, with larger circles indicating higher cell numbers. Cells expressing ligands are denoted with arrows pointing towards cells expressing receptors. The thicker the line, the more ligand-receptor pairs there are. B: Cell-to-cell interaction probability/strength network in the Normal and Sepsis groups. The strength is calculated by summing the probability values. C: Cell interaction bubble plot in the Normal group. D: Cell interaction bubble plot in the Sepsis group. E: Signal reception system analysis of the communication network in the Normal and Sepsis groups. F: Signal emission system analysis of the communication network in the Normal and Sepsis groups.

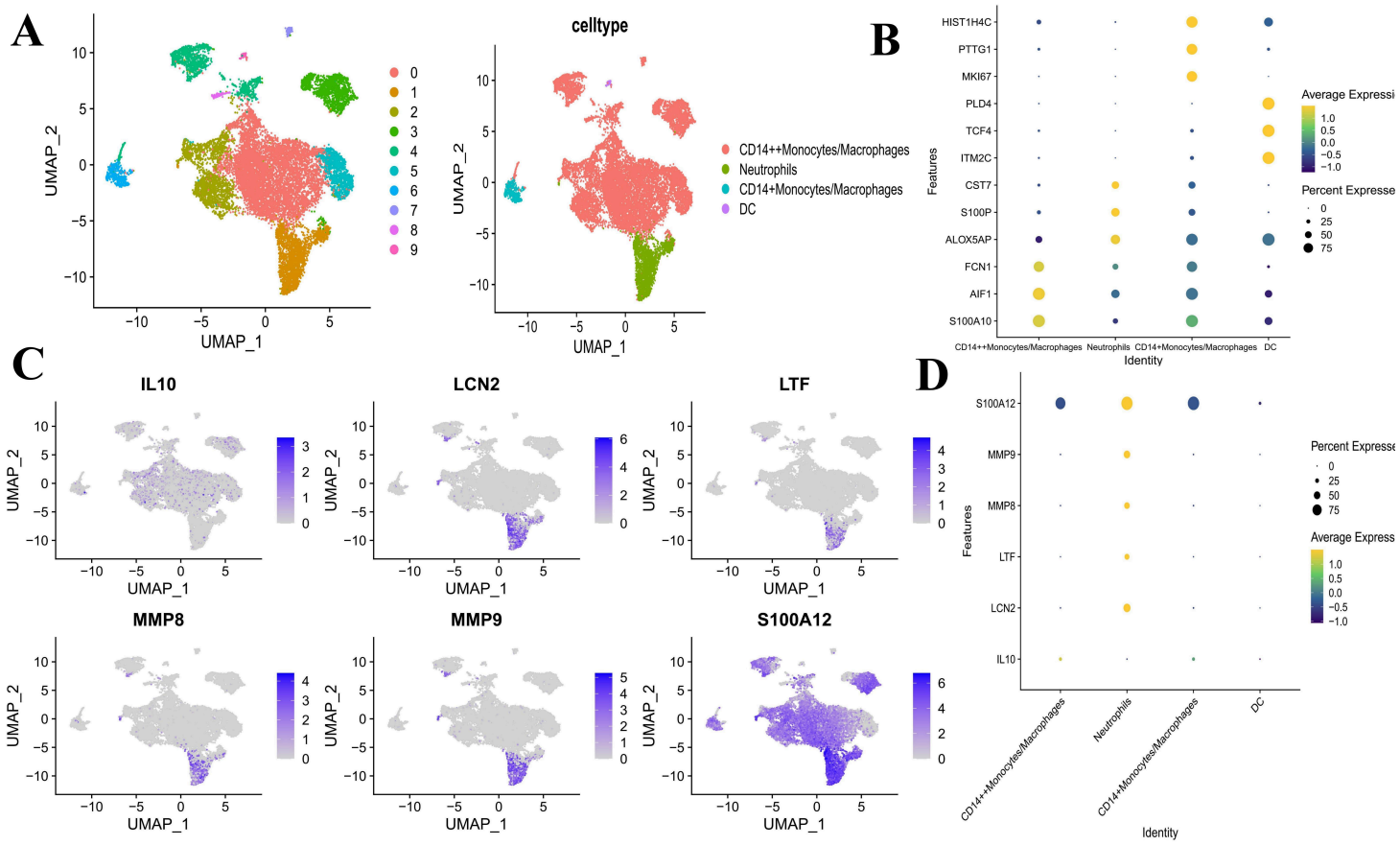


Figure 4

Single-Cell Myeloid Cell Subpopulation Annotation, Marker Gene Localization, and Pseudotime Analysis in Sepsis

A: Re-clustering and annotation of myeloid cell subpopulations. B: Bubble plot of marker gene expression across myeloid cell subpopulations. C: UMAP plots showing the expression distribution of six biomarkers in myeloid cells. D: Bubble plot of six biomarker expression in different myeloid cell subpopulations.

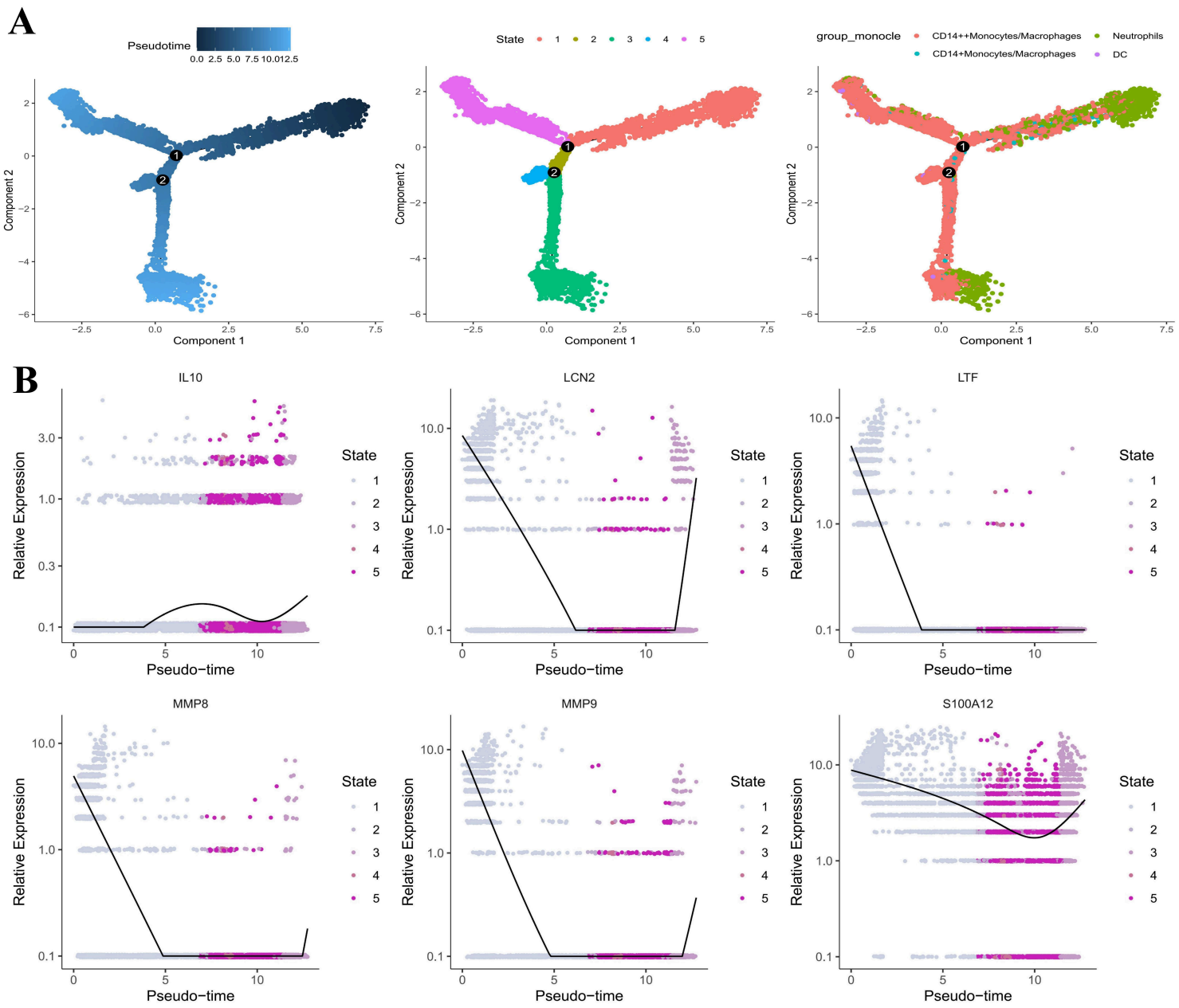


Figure 5

Pseudotime analysis of Myeloid cells subtypes and their gene expression dynamics

A: Pseudotime trajectory analysis of Myeloid cells. B: Expression patterns of key genes during pseudotime progression.

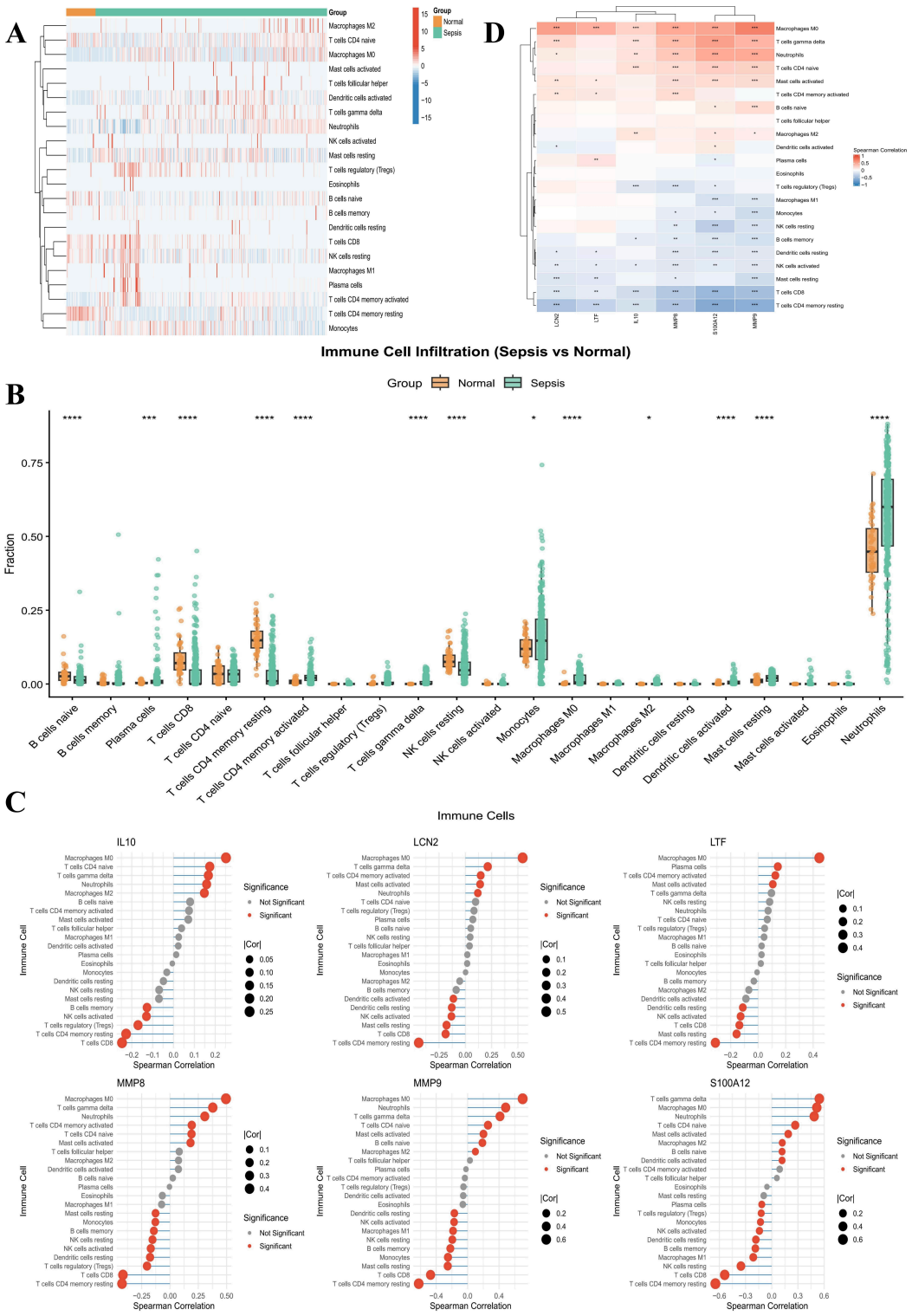


Figure 6

Immune Cell Infiltration Analysis in Sepsis vs. Normal Groups A：Heatmap of Immune Cell Infiltration. B：Boxplot of Immune Cell Infiltration. C：Spearman Correlation of Immune Cells with Gene Expression. D. Heatmap of Immune Cell Correlations.